Fabrication of Holographic Gratings in As_2S_3 Glass by Photoexpansion and Photodarkening

S. Ramachandran, S. G. Bishop, *Member, IEEE*, J. P. Guo, *Member, IEEE*, and D. J. Brady, *Member, IEEE*

***Abstract*—The spatial dynamics of the photo-induced surface relief and phase gratings in As_2S_3 glass are described. Excursion amplitudes up to 150 nm and grating efficiencies up to 27% are observed. Depth and resolution limits for the effect are measured and a model for the resolution limit is proposed.**

OPTICAL ELEMENTS for applications in communications, interconnections and data storage can be patterned in chalcogenide glasses by illumination with above band gap light, which causes photodarkening [1], [2] and photoexpansion [3]. Photodarkening [4] is a photo-induced red shift of the optical absorption edge and is accompanied by an increase in the index of refraction in the transparent spectral range below the absorption edge. Photoexpansion [4]–[6] is an increase in the volume of a photodarkened chalcogenide glass. Stress relaxation at the interface between darkened and unexposed regions due to volume differences [3] can cause expansions as large as 2%. Hisakuni *et al.* [7] used photoexpansion to fabricate lenslets on the surface of As_2S_3 glass.

The present work uses photodarkening and photoexpansion effects to holographically record diffraction gratings in bulk As_2S_3 glass. Diffraction efficiency measurements and atomic force microscope (AFM) images of the gratings demonstrate that photoexpansion creates a surface relief grating on the glass, while the attendant photodarkening induces a phase grating due to index variations under the surface of the glass. Measurement of the diffraction efficiency as successive layers are removed from the surface of the grating by polishing allows us to assess the influence of the index modulation on the overall diffraction efficiency and to determine the effective depth of the index change induced by the photodarkening effect. Theoretically predicted values of Raman–Nath diffraction efficiencies were compared with experimentally observed values to separately characterize the surface gratings and the bulk (index) gratings. Gratings were written for different exposures and periods, and AFM images reveal a resolution limit of 0.70 μm for the fabrication of surface gratings with the photoexpansion effect. Stress analysis models are used to explain this resolution limit. To the best of our knowledge, this is the first reported fabrication of surface diffractive optic structures using photoexpansion in bulk chalcogenide glass. Working in the bulk provides information on index profiles at depths well beyond the thicknesses of typical thin films. Photodarkening parameters such as the required exposure and the maximum attainable index change depend on the thermal anneal cycles to which an evaporated or sputtered thin film is subjected. However, bulk glasses do not differ in the anneal cycles and consequently the photodarkening parameters show little batch to batch variation.

One-inch diameter disks of As_2S_3 glass, with a thickness of 1.25 mm, were obtained from Amorphous Materials Inc. [8]. Gratings were recorded holographically using a TE polarized Argon ion laser operating at $\lambda = 514.5$ nm. The laser beam was spatially filtered and collimated as a plane wave with a radius of 1.5 cm. This beam was split into two beams that form an interference pattern at the surface of the glass. The stability of this set up was measured by constructing an interferometer, with a CCD camera measuring the time averaged modulation depth for an interference pattern. The visibility of the resultant interference pattern, defined as

$$V = \left\langle \frac{I_{\max} - I_{\min}}{I_{\max} + I_{\min}} \right\rangle \tag{1}$$

where $I_{\max}$ and $I_{\min}$ are the maximum and minimum intensities on the interference pattern, was 0.60 for a 60 min. long exposure. In (1), the symbol $\langle\ \rangle$, stands for a time average. The absorption coefficient in As_2S_3 glass at this wavelength is [9] 1700 cm^{-1}, and is well suited for photodarkening applications. The grating diffraction efficiency was monitored using a TE polarized He–Ne probe laser operating at 632.8 nm. Light at this wavelength is only weakly absorbed ($\alpha = 0.37$ cm^{-1} at $\lambda = 632.8$ nm) in As_2S_3 glass [8] and the probe was highly attenuated to avoid influencing the photodarkening process. The benign role of the probe beam was confirmed by probing recorded gratings with the He-Ne beam over a period of 12 hours. No change was observed in the diffraction efficiency of the gratings. Photodarkening by the He–Ne laser beam would have caused a monotonic decrease in diffraction efficiency.

The first set of gratings was made with a writing angle of 5.0°. For 514.5 nm light, this corresponds to a grating period of 2.95 μm. Power densities of the split recording beams were identical at 0.17 W/cm^2 resulting in a peak power density of 0.65 W/cm^2 in the regions of maximum constructive interference. Gratings with exposure times varying from 5 min. to 60 min. were recorded. The first-order diffraction efficiency was measured during the exposure with the He–Ne probe beam.

Manuscript received February 9, 1996; revised April 29, 1996. This work was supported by ARPA under the Center for Optoelectronic Science and Technology Program (Grant #MDA972-94-1-0004) and by NSF under the Engineering Research Center Program (NSF ECD 89-43166).

The authors are with the Center for Optoelectronic Science and Technology, Center for Compound Semiconductor Microelectronics, and Department of Electrical and Computer Engineering, University of Illinois at Urbana-Champaign, Urbana, IL 61801 USA.

Publisher Item Identifier S 1041-1135(96)05835-1.

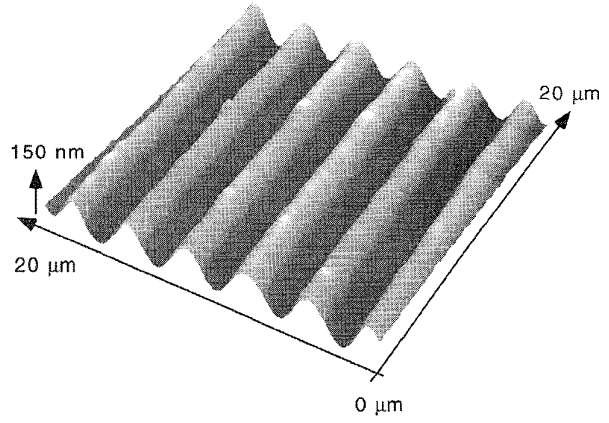

Fig. 1. AFM scan of a grating, holographically written with a total exposure of 2.3364 kJ/cm^2. Grating period = 2.95 μm. A peak to valley height of 145 nm was measured and the diffraction efficiency of this grating was 27.39%.

Fig. 1 is an AFM image of a 2.95 μm period grating written with an exposure of 2.3 kJ/cm^2. The excursion amplitude for this grating was 145 nm and a diffraction efficiency of 27.39% was observed. Gratings that were fabricated with doses higher than 2.3 kJ/cm^2 revealed no increase in excursion amplitudes, implying that this dosage corresponds to a saturation value.

To test the resolution limit of the photoexpansion process for the formation of surface structures, gratings with periods varying from 2.95 μm to 0.38 μm were fabricated. Higher frequency gratings were obtained by increasing the writing angle of the argon ion laser beams. Increases in Fresnel reflection were off-set by increasing the exposure times. The dosage at regions of maximum constructive interference was fixed at the saturation value of 2.3 kJ/cm^2. Diffraction efficiency measurements at Bragg incidence and AFM scans to measure the amplitudes of surface relief were obtained for every grating fabricated. Fig. 2 shows line scans through the AFM images of gratings fabricated with different periods. Note that the excursion amplitude for the relief structure decreases with decreasing grating period. Gratings with periods as low as 0.3 mm (not shown in Fig. 2) had a diffraction efficiency of 0.07% but had no measurable surface structure. Previous studies [10] report no evidence of a resolution limit for index gratings written in As_2S_3 glass. This suggests that only the surface gratings are resolution limited.

The relief gratings had excursion amplitudes less than 200 nm and thus could be analyzed as thin [11] gratings operating in the Raman–Nath regime. The first order efficiency of Raman–Nath diffraction for a probe beam tuned to the Bragg condition is given by

$$\eta = J_1^2(2\gamma) \tag{2}$$

where J_1 is the first-order Bessel's function, and γ is the grating strength parameter, given by

$$\gamma = \frac{\pi \Delta n d}{\lambda \cos\theta} \tag{3}$$

where d is the thickness of the hologram, Δn is the amplitude of index perturbation, and θ is the (Bragg) angle of incidence of the probe (He–Ne) beam. For relief gratings, Δn is the

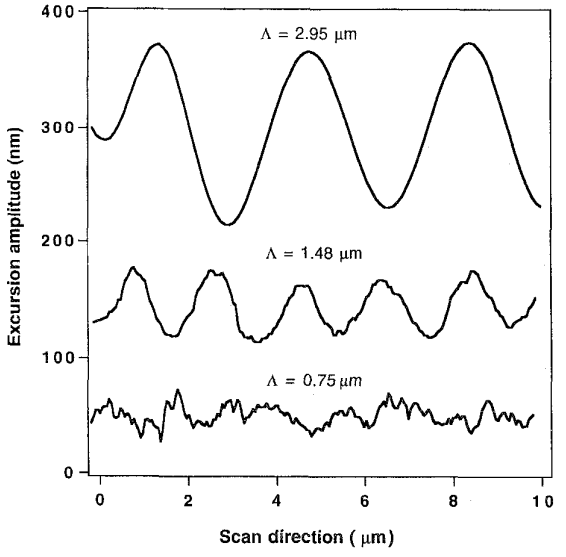

Fig. 2. Line scans through AFM images of gratings fabricated at different frequencies. The grating period, Λ, is labeled next to each scan line. The grating excursion amplitude decreases as the grating period is decreased.

TABLE I
COMPARISON OF EXCURSION AMPLITUDES, AND OBSERVED AND THEORETICALLY PREDICTED DIFFRACTION EFFICIENCIES FOR GRATINGS WITH DIFFERENT WRITING TIMES AND PERIODS. SURFACE RIPPLE AMPLITUDE INCREASES WITH EXPOSURE TIME BUT DECREASES WITH INCREASING GRATING FREQUENCY. ALSO INDEX (BULK) GRATINGS PLAY AN INCREASINGLY DOMINANT ROLE AS GRATING FREQUENCY IS INCREASED

Grating Period (μm)	Exposure (Joules/cm^2)	Peak to valley height (nm)	First order diffraction efficiency (%)	
			measured	Raman-Nath theory
0.377	2336.4	0	0.07	0
0.750	2336.4	18.8	1.40	0.63
1.48	2336.4	49.9	3.50	3.94
2.95	2336.4	145.0	27.39	23.88
	1168.2	107.1	12.30	15.30
	584.1	75.8	10.00	8.42

difference between the indices of air and glass. Values for d were obtained from AFM scans. Table I shows the surface grating thickness, d, and the corresponding theoretically expected and experimentally observed diffraction efficiencies for select gratings. The theoretically expected diffraction efficiencies are calculated from (2) and reflect the expected contribution from the surface gratings only. The dose applied for each grating is also shown, to differentiate between the three gratings with 2.95-μm period. Table I indicates that the theoretical predictions closely correspond to the experimental observations of the diffraction efficiency for the three gratings with 2.95-μm period. This means that almost all of the diffraction observed for gratings with large period is due to the surface gratings alone.

To test the index variation due to photodarkening as a function of grating depth, we polished layers off the surface of the grating in 2-μm increments. Fig. 3 is a plot of diffraction efficiency versus polishing depth for the grating shown in Fig. 1. The diffraction efficiency drops sharply upon removing the surface layer, consistent with the theoretical predictions of Table I that the majority of diffraction observed is due to the surface modulation. Since the amplitude of index

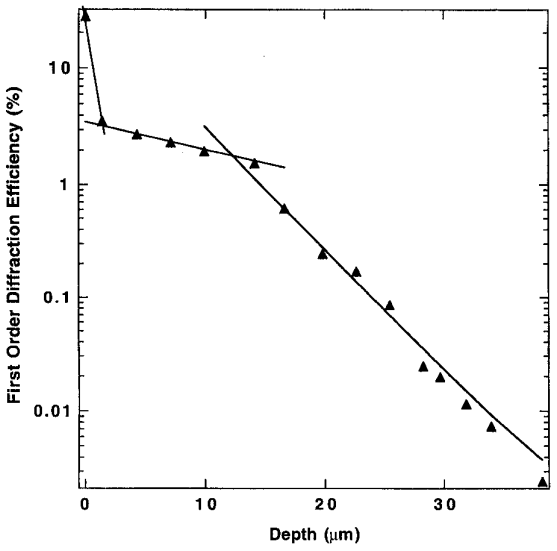

Fig. 3. Depth profile of diffraction efficiency on 2.95 μm period gratings indicating the existence of a thick holographic index grating. The diffraction efficiency drops sharply once the surface grating is removed. Profile indicates two regimes of index gratings—the saturated index region and a region where the index modulation amplitude decreases.

modulation due to photodarkening is expected to be much smaller than that for the surface gratings, the contribution to the overall diffraction efficiency due to the index gratings is relatively weak. This contrasts with reported values [12] of diffraction efficiencies which are as high as 70% in thin films of As_2S_3 glass. To the best of our knowledge, reports of gratings in chalcogenide glasses have been limited to thin films where metastable structures can give rise to irreversible as well as reversible photo-induced index changes as great as 5%. No relief grating structures have been observed in thin films. A direct comparison of results in thin films and bulk material is obscured by strong dependence of the photoresponse on preparation technique of thin films. It appears that photo-induced index changes are relatively weak in bulk chalcogenide glasses owing to a stabler bond structure. The relatively slow drop in diffraction efficiency in the intermediate region reveals a saturated index front that extends up to 15 mm beneath the surface.

The characteristics of the gratings shown in Fig. 2 are listed in Table I. The peak to valley height of the surface gratings decreases monotonically, with increasing grating frequency. No observable surface features were found on gratings with periods less than 0.70 μm. Raman–Nath diffraction efficiency values tabulated in Table I indicate that the contribution to the total diffraction efficiency from surface gratings decreases as grating frequency increases. This means that even though the relief gratings diminish in strength, increasing grating frequency does not decrease the contribution from index gratings, consistent with previous observations [10] that index gratings show no observable resolution limit in chalcogenide glasses. Therefore, it appears that the resolution of gratings produced as a consequence of the two phenomena, namely photodarkening and photoexpansion, are different, even though they have the same physical origin.

The difference between photodarkening and photoexpansion is resolved by considering the process of surface dilation. While index changes are caused by photo-induced changes in local bonds, the surface expansion occurs due to strain relaxation over many bonds. The mechanical stress field that leads to this relaxation is not limited to the region that was irradiated. Hence, the surface dilation extends beyond the region that was illuminated. Consequently, when two such regions are brought in proximity, the dilations of the two regions superpose and the dc value of the surface modulation increases. We postulate that in the case of the grating with 2.95-μm period, the observed 150 nm modulation amplitude is superimposed on a dc surface dilation. As the grating period is decreased, the degree of overlap between adjacent expanding regions increases and in the case of the grating with 0.377-μm period, the surface ripple is totally obliterated by this overlap and photoexpansion contributes to a dc surface dilation only.

In summary, we have used the photoexpansion effect to demonstrate fabrication of surface grating structures in chalcogenide glasses with peak to valley heights of up to 150 nm. We determined a resolution limit of 0.70 mm, for grating structures written at saturated exposures of above band-gap light for As_2S_3 glass. The exposure dependence of the height and lateral spread for relief grating structures has been explained using the photoexpansion effect in conjunction with a model for stress relaxation. It is found that mechanical stress relaxation phenomena play an important role in determining the height and locality of surface expanded structures.

ACKNOWLEDGMENT

The authors would like to thank P. C. Taylor for helpful discussions. The AFM images were obtained at the Beckman Institute Visualization Lab.

REFERENCES

[1] H. Nishihara, M. Haruna, and T. Suhara, "Optical Integrated Circuits," in *McGraw-Hill Optical and Electro-Optical Engineering Series*, R. E. Fisher and W. E. Smith, Eds. New York: McGraw-Hill, 1989, pp. 151–154, 215.

[2] J. P. DeNeufville, S. C. Moss, and S. R. Ovshinsky, "Photostructural transformations in amorphous As_2Se_3 and As_2S_3 films," *J. Non-Cryst. Solids*, vol. 13, pp. 191–223, 1973/1974.

[3] H. Hisakuni and K. Tanaka, "Giant photoexpansion in As_2S_3 glass," *Appl. Phys. Lett.* vol. 65, pp. 2925–2927, 1994.

[4] Y. Utsugi and Y. Mizumisha, "Lattice dynamical aspects of photoexcited chalcogenide glasses," *Jpn. J. Appl. Phys.-Pt. 1*, vol. 31, pp. 3922–3933, 1992.

[5] K. Tanaka, "Photoinduced structural changes in chalcogenide glasses," *Rev. Solid State Sci.*, vol. 4, pp. 641–659, 1990.

[6] H. Hamanaka, K. Tanaka, A. Matsuda, and S. Iizima, "Reversible photoinduced volume changes in evaporated As_2S_3 and $As_4Se_5Ge_1$ films", *Solid State Commun.*, vol. 19, pp. 499–501, 1976.

[7] H. Hisakuni and K. Tanaka, "Optical fabrication of microlenses in chalcogenide glasses," *Opt. Lett.*, vol. 20, pp. 958–960, 1995.

[8] Amorphous Materials Inc., Garland TX, materials specification.

[9] J. Tauc, A. Menth, and D. L. Wood, "Optical and magnetic investigations of the localized states in semiconducting glasses," *Phys. Rev. Lett.*, vol. 25, pp. 749–52, 1970.

[10] A. Singh, R. A. Lessard, and M. Samson, "Effect of temperature on diffraction efficiency of holograms recorded in arsenic trisulphide thin films," *Optica Acta*, vol. 31, pp. 1161–1165, 1984

[11] T. K. Gaylord and M. G. Moharam, "Analysis and applications of optical diffraction by gratings," *Proc. IEEE*, vol. 73, pp. 894–937, 1985.

[12] S. A. Keneman, "Hologram storage in arsenic trisulphide thin films," *Appl. Phys. Lett.*, vol. 19, pp. 205–207, 1971.